Longitudinal and Lateral Vibration Analysis of Cables in a Cable Robot using Finite Element Method

H. Tourajizadeh*
Department of Mechanical Engineering,
University of Kharazmi, Iran
*Corresponding author, E-mail: Tourajizadeh@khu.ac.ir

M. Yousefzadeh, M. H. Korayem
Department of Mechanical Engineering,
Iran University of Science and Technology, Iran
E-mail: myousefzadeh@iust.ac.ir / hkorayem@iust.ac.ir

Abstract: In this paper, vibrational response of a variable-length cable in longitudinal, lateral and torsional directions is analysed in a cable robot using FE method. The flexibility of cables has remarkable effect on positioning of the end-effector in cable robots. Also considering the fact that the length of the cables are time dependent in a dynamic cable structure like robocrane, the numerical approaches are preferable compared to analytic solutions. To do so, the cable is divided into finite elements in which the virtual work equation and Galerkin method can be implemented for the equations. Considering the stiffness matrix, the characteristic equations and Eigen values of each element can be defined. A simulation study is done in the ANSIS on a planar robocrane with 2-DOF and also for a spatial case with 6-DOF that is controlled by the aid of six variable-length flexible cables in the space for two different types of solid and flexible end-effectors. Whole the cable robot flexibility is analyzed simultaneously instead of separation calculation of each cable. Not only all of the 3-D vibrating behaviour of the whole structure is studied in this paper but also the lengths of the cables are considered as variable. The vibrating response of mode shapes, amplitude and frequencies are extracted and analysed, and the results are compared for two case of solid and flexible end-effector which shows the effect of the flexibility in the position of the end-effector and the tension of the cables in different situations.

Biographical notes: H. Tourajizadeh received his MSc from Iran Univ. of Science and Tech. in 2008 in applied mechanical design. He is currently a PhD candidate in IUST with a number of research publications. His research interests include robotic, automotive eng., control and optimization, and mechatronic systems. **M. Yousefzadeh** received his BSc in Mechanical Engineering in 2000 and his MSc in 2003 in the field of automotive system design. He is currently a PhD student in Iran University of Science and Technology in the field of control. He has 12 years of experience in special machinery design for automotive industry and teaching experience in different universities. **M. Habibnejad** Korayem received his MSc in Mech. Eng. from Amirkabir Univ. of Tech. in 1987. He obtained his PhD in Mech. Eng. from Univ. of Wollongong, Australia, in 1994. He is a Professor in Mech. Eng. at IUST.

1   INTRODUCTION

Cable robots are one of the new generations of parallel robots in which the end-effector is controlled by the aid of several cables that just can exert tensional force to the end-effector. The applied cables which are used as the actuator of the end-effector should be flexible enough to provide the possibility of its rotation around a drum without forming a rotational spring on the drum which is a negative drawback on the calculated kinematic and kinetic of the robot. That's why a little flexibility of the cables is unavoidable. Increasing the inertial forces of the End-effector and cables leads to considerable deformation in the cables and consequently generates significant vibrational error on the position of the end-effector which influences the accuracy of the robot. Hence, vibration of the cables is the most challenging problem in controlling of such robots which can cause enormous deviation in the position of the end-effector [1, 2]. Both of axial and transversal flexibilities appear in these cables. Cable robots are manufactured under two main categories: Under-constrained and Fully-constrained.

According to an analytic research on a fully-constrained cable robot, the transversal flexibility is ignorable compared to the axial flexibility [3]. However this assumption is not completely valid for under-constrained robots. Cable suspended robots which are under-constrained are so popular since they do not have limited work space [4, 5]. The most important challenge in order to analyse the vibrational response of such cables is their variable length during the dynamic process of the robot which makes it difficult to solve their PDE using ordinary solutions. In previous researches continuum and multi dynamic models of cables were used for vibrational modelling. Authors in [6] present a procedure for studying the dynamics of a single variable length cable system. The cable is modelled as a chain and is treated as a multibody system. The chain links in turn are modelled as lumped masses. Here the dynamic is extracted for a single cable. Some vibrating analysis of elastic cable robots can be found in [7].

This paper discusses a feedback control method for incompletely restrained wire-suspended mechanisms and anti-sway control method with exact linearization using inverse dynamics is designed for incompletely restrained type mechanism. Here since the cable is incompletely restrained, the vibration and swing is unavoidable which is neutralized using the mentioned controlling strategy. Again the modelling and simulation is done for a single rope. Dynamic and control of a complete robocrane actuated by seven cables is studied in [8] however the important problem of flexibility of the cables is ignored here. Workspace study of these kinds of robocranes is done in [9] in which again the effect of flexibility is not considered in the obtained workspace. Another research of solid robocrane is done in [10] in which a different method of controlling of the cable robots is presented using active boundary control. Since the vibrating analysis of cables using analytic methods, especially for the time dependent length versions is extremely difficult, numerical algorithms are preferred in some literatures. Vibration analysis of a single cable with a constant length is done in [11] using the FE method, and it is extended in [12] for the variable-length one. FEM and FEA are used together in order to analyze the dynamic and planar vibration of a cable in [13]. Vibration analysis of the cables used in a simple structure is done in [14]. For the mentioned researches again the numerical methods are employed for a single cable which does not show the effect of flexibility of a complete dynamic cable structure like robocranes on deviation of their end-effectors.

Therefore, considering the mentioned shortage in the literatures, in this paper flexibility analysis of a dynamic cable structure like cable robots is extracted for time-variable length cables using numerical finite element approach by which the effect of the flexibilities can be easily investigated on the deviation of the robot end-effector. Galerkin method is used here in both longitudinal and lateral directions. This calculation is done for whole of the cables and their structure simultaneously instead of analyzing each cable separately. FEM is chosen here since a fast calculation with an acceptable accuracy could be provided for a variable length case. Since the studied cable robot is under-constrained, both of lateral and longitudinal vibrations need to be analyzed simultaneously for the robot with time variable cables' length. This study is first done for a three-cable planar robot with two degrees of freedom and it is then extended for a 6-cable spatial robot with six degrees of freedom. Dynamic formulation of the planar structure can be found in [15, 16] while the spatial case is presented in [17].

First of all, dynamic modelling of a single cable rope is extracted using Lagrangian method which results in longitudinal, lateral and torsional vibration equations of the cable. Afterwards, resultant differential equations are solved using weighted residual functions and the Galerkin method. Using the finite-element method, the rope is divided into finite elements which give us the shape functions, stiffness matrix, characteristic equation of the system and finally Eigen values or natural frequencies of the vibration of the system. This process is then extended for a six-cable robot with variable length cables. Correctness of the presented

theoretical formulations is investigated using a simulation study for both of planar and spatial samples of cable robots. A 3-cable robot with a massive end-effector and two degrees of freedom is first modeled in the ANSYS and then it is extended for a six cable triangular end-effector with six degrees of freedom.

The first simulation analyses the planar vibrations of the cable while the second one covers the vibration of the cables in three directions. Also an interesting comparison is performed for a robot structure in which the end-effector's vibration is ignorable compared to the cable's vibration and the structure in which the end-effector is also flexible. Natural frequencies, mode shapes and maximum stress of the cables for all of the mentioned systems are gained and analyzed. Results show that cable vibrations can affect the position of the end-effector in the systems which are not equipped with a suitable controller especially for the spatial case.

2   DYNAMIC FORMULATION

First the formulation of a single cable is represented. Considering a cable composed of several twisted ropes like Fig. 1 results in longitudinal elongation [18], Here Θ is rotational flexibility of the cable, U is its longitudinal flexibility along *Z* axis, *f* and *q* are force and torque of the cable respectively, *T* is the tension of the cable at position *S* and *C* is torsional stress of the cable.
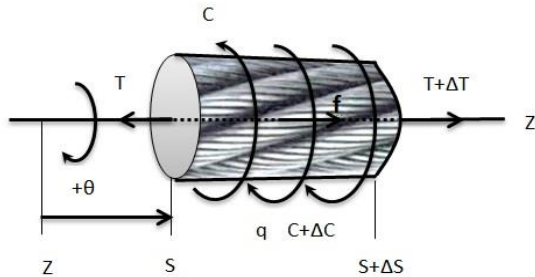
Fig. 1   Schematic of a single rope [18]

Using Lagrangian method, the following dynamic equations can be achieved which include two parameters of angular and longitudinal displacement:

$$m\omega^2 U + k_1 U_{xx} + K_2 \Theta_{xx} = 0$$
$$I\omega^2 \Theta + k_3 U_{xx} + k_4 \Theta_{xx} = 0 \tag{1}$$

where *m* and *I* are the mass and inertia of the cable respectively, K_i is flexibility coefficient of the rope, ω is time derivation of rotational flexibility and the index *x* indicates derivation respect to *S*.

Implementation of weighted residual function and Galerkin method results in the following differential equations:

$$W_U = \int_0^L \delta U(m\omega^2 U + k_1 U_{xx} + K_2 \Theta_{xx})dx = 0$$

$$W_\Theta = \int_0^L \delta\Theta(I\omega^2 \Theta + k_3 U_{xx} + k_4 \Theta_{xx})dx = 0 \tag{2}$$

Dividing the cable into finite elements and using partial integral, we have:

$$W^e_U = \int_0^L U(\frac{k_1 \delta U_{\zeta\zeta}}{l^2} + m\omega^2 \delta U)ld\zeta - [\frac{k_1}{l}\delta U_\zeta U]\Big|_0^l - \int_0^l \frac{k_2}{l}\delta U_\zeta \Theta_\zeta d\zeta$$

$$W^e_\theta = \int_0^L U(\frac{k_4 \delta\Theta_{\zeta\zeta}}{l^2} + I\omega^2 \delta\Theta)ld\zeta - [\frac{k_4}{l}\delta\Theta_\zeta \Theta]\Big|_0^l - \int_0^l \frac{k_2}{l}\delta\Theta_\zeta U_\zeta d\zeta \tag{3}$$

Shape functions can be defined as:

$$U(\zeta) = \langle N_{1a} N_{2a} \rangle \begin{Bmatrix} U_1 \\ U_2 \end{Bmatrix}$$

$$\Theta(\zeta) = \langle N_{1r} N_{2r} \rangle \begin{Bmatrix} \Theta_1 \\ \Theta_2 \end{Bmatrix} \tag{4}$$

By supposing the shape functions as below:

$$U(\zeta) = C_1 sin(\sigma\zeta) + C_2 cos(\sigma\zeta); \sigma = \omega L\sqrt{m/k_1}$$

$$\Theta(\zeta) = D_1 sin(\eta\zeta) + D_2 cos(\eta\zeta); \eta = \omega L\sqrt{I/k_4} \tag{5}$$

The final resultant shape functions are:

$$\begin{cases} N_1(\omega)_a = \dfrac{sin(\alpha L(1-\zeta))}{sin(\alpha L)} \\[2mm] N_2(\omega)_a = \dfrac{sin(\alpha L\zeta)}{sin(\alpha L)}; \\[2mm] \alpha = \omega\sqrt{m/k_1} \end{cases} \tag{6}$$

$$\begin{cases} N_1(\omega)_r = \dfrac{sin(rL(1-\zeta))}{sin(rL)} \\[2mm] N_2(\omega)_r = \dfrac{sin(rL\zeta)}{sin(rL)} \\[2mm] ; r = \omega\sqrt{I/k_4} \end{cases}$$

By substituting the mentioned shape functions into the weighted residual function equations, we have:

$$W_U^e = \left\langle \delta U_1 \delta U_2 \right\rangle \begin{pmatrix} \dfrac{K_1}{l} \begin{bmatrix} -N'_{1\alpha\xi=0} & N'_{1\alpha\xi=1} \\ -N'_{2\alpha\xi=0} & N'_{2\alpha\xi=1} \end{bmatrix} \begin{bmatrix} u_1 \\ u_2 \end{bmatrix} + \\ \dfrac{K_2}{l} \int_0^l \begin{bmatrix} N'_{1\alpha}N'_{1\tau} & N'_{1\alpha}N'_{2\tau} \\ N'_{2\alpha}N'_{1\tau} & N'_{2\alpha}N'_{2\tau} \end{bmatrix} d\zeta \begin{bmatrix} \Theta_1 \\ \Theta_2 \end{bmatrix} \end{pmatrix}$$

$$W_\Theta^e = \left\langle \delta \Theta_1 \delta \Theta_2 \right\rangle \begin{pmatrix} \dfrac{K_4}{l} \begin{bmatrix} -N'_{1\tau\xi=0} & N'_{1\tau\xi=1} \\ -N'_{2\tau\xi=0} & N'_{2\tau\xi=1} \end{bmatrix} \begin{bmatrix} \Theta_1 \\ \Theta_2 \end{bmatrix} + \\ \dfrac{K_2}{l} \int_0^l \begin{bmatrix} N'_{1\tau}N'_{1\alpha} & N'_{1\tau}N'_{2\alpha} \\ N'_{2\tau}N'_{1\alpha} & N'_{2\tau}N'_{2\alpha} \end{bmatrix} d\zeta \begin{bmatrix} u_1 \\ u_2 \end{bmatrix} \end{pmatrix} \tag{7}$$

where:

$$W^e = \left\langle \delta u_n \right\rangle \big[k(\omega) \big]_{4*4}^e \{ u_n \}_{4*1};$$

$$\big[k(\omega) \big]^e = \big[k(\omega) \big]_{uncoupled}^e + \big[k(\omega) \big]_{coupling}^e \tag{8}$$

Galerkin results in the following general characteristic equation:

$$W = \sum_{elements} W^k = \left\langle \delta U_n \right\rangle \big[K(\omega) \big] \{ U_n \} = 0 \tag{9}$$

Natural frequencies of the system can be obtained by the aid of mentioned characteristic equation. The same procedure can be done for a six-cable robocrane of the Fig. 2.
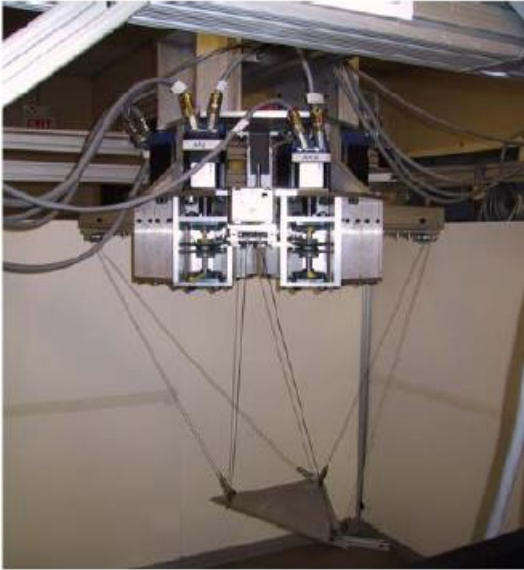
Fig. 2   Scheme of a spatial cable robot [19]

Here six DOFs of the lower triangular end-effector plate are controlled using six flexible cables connected to the upper triangular fixed plate. The lengths of the cables are time dependent which makes it difficult to

use analytical methods for analysing their flexibilities. First of all dynamic equation of the system is extracted using Hamiltonian method. Kinetic and potential energies of the system are calculated without considering any external forces:

$$T = 1/2\rho\left(\left(\frac{\partial u}{\partial t} \right)^2 + \left(\frac{\partial v}{\partial t} \right)^2 \right) + 1/2I\left(\left(\frac{\partial \theta}{\partial t} \right)^2 \right)$$

$$V = 1/2AE\left(\left(\frac{\partial^2 u}{\partial x^2} \right)^2 + \left(\frac{\partial^2 v}{\partial x^2} \right)^2 \right) + 1/2k\left(\left(\frac{\partial^2 \theta}{\partial x^2} \right)^2 \right) \tag{10}$$

where u, v and θ are longitudinal, lateral and torsional displacement of the cables respectively. Also ρ is the density, E is the elasticity module and A is the cross section area of the cables. Using Hamiltonian formulation, the following dynamic equations can be presented:

$$\int \delta(T-V)dt = 0$$

$$\begin{cases} \rho \dfrac{\partial^2 u(x,t)}{\partial t^2} + k_{11} \dfrac{\partial^2 u(x,t)}{\partial x^2} + \\ k_{12} \dfrac{\partial^2 v(x,t)}{\partial x^2} + k_{13} \dfrac{\partial^2 \theta(x,t)}{\partial x^2} = 0 \\ \rho \dfrac{\partial^2 v(x,t)}{\partial t^2} + k_{21} \dfrac{\partial^2 u(x,t)}{\partial x^2} + \\ k_{22} \dfrac{\partial^2 v(x,t)}{\partial x^2} + k_{23} \dfrac{\partial^2 \theta(x,t)}{\partial x^2} = 0 \\ \rho \dfrac{\partial^2 \theta(x,t)}{\partial t^2} + k_{31} \dfrac{\partial^2 u(x,t)}{\partial x^2} + \\ k_{32} \dfrac{\partial^2 v(x,t)}{\partial x^2} + k_{33} \dfrac{\partial^2 \theta(x,t)}{\partial x^2} = 0 \end{cases} \tag{11}$$

In order to use the weighted residual method, the following functions are chosen:

$$\begin{cases} u(x,t) = U(x)\sin \omega t; \\ v(x,t) = V(x)\sin \omega t; \\ \theta(x,t) = \theta(x)\sin \omega t \end{cases} \tag{12}$$

Substituting the above functions in the dynamic equations, vibrating formulations can be defined as below:

$$\begin{cases} m\omega^2 U + k_{11}U_{xx} + k_{12}V_{xx} + k_{13}\theta_{xx} = 0; \\ m\omega^2 V + k_{21}U_{xx} + k_{22}V_{xx} + k_{23}\theta_{xx} = 0; \\ m\omega^2 U + k_{31}U_{xx} + k_{32}V_{xx} + k_{33}\theta_{xx} = 0 \end{cases} \tag{13}$$

Using the weighted residual method, the following virtual work formulation can be gained, which defines the vibrating amplitude:

$$\begin{cases} W_U = \int\limits_0^{L(t)} \delta U(m\omega^2 U + k_{11}U_{xx} + k_{12}V_{xx} + k_{13}\theta_{xx})dx = 0; \\[2mm] W_V = \int\limits_0^{L(t)} \delta V(m\omega^2 V + k_{21}U_{xx} + k_{22}V_{xx} + k_{23}\theta_{xx})dx = 0; \\[2mm] W_\theta = \int\limits_0^{L(t)} \delta\theta(m\omega^2 \theta + k_{31}U_{xx} + k_{32}V_{xx} + k_{33}\theta_{xx})dx = 0 \end{cases} \tag{14}$$

3 STIFFNESS MATRIX CALCULATION

Now we can divide the cable into finite longitudinal elements with two nodes and three degrees of freedom. Considering boundary condition, the following virtual work formulation can be obtained:

$$\begin{cases} W_U^e = \int\limits_0^1 (-\dfrac{\delta U_\zeta}{l^2}(k_{11}U_\zeta + k_{12}V_\zeta + k_{13}\theta_\zeta) + \delta U m\omega^2 U)ld\zeta; \\[2mm] W_V^e = \int\limits_0^1 (-\dfrac{\delta V_\zeta}{l^2}(k_{21}U_\zeta + k_{22}V_\zeta + k_{23}\theta_\zeta) + \delta V m\omega^2 V)ld\zeta; \\[2mm] W_\theta^e = \int\limits_0^1 (-\dfrac{\delta\theta_\zeta}{l^2}(k_{31}U_\zeta + k_{32}V_\zeta + k_{33}\theta_\zeta) + \delta\theta m\omega^2 \theta)ld\zeta \end{cases} \tag{15}$$

According to the mentioned equations, Galerkin equations produce the following weighted functions which are the vibrating amplitude of the system:

$$\begin{cases} U(\zeta) = U_1 \sin(\sigma\zeta) + U_2 \cos(\sigma\zeta); \\ \sigma = \omega L(t)\sqrt{m/k_{11}}; \\ V(\zeta) = V_1 \sin(\eta\zeta) + V_2 \cos(\eta\zeta); \\ \eta = \omega L(t)\sqrt{m/k_{22}}; \\ \theta(\zeta) = \theta_1 \sin(\mu\zeta) + \theta_2 \cos(\mu\zeta); \\ \mu = \omega L(t)\sqrt{m/k_{33}} \end{cases} \tag{16}$$

Vibrating amplitudes are definable according to the shape function as below:

$$\begin{cases} U(\zeta) = \begin{pmatrix} N_{1U} & N_{2U} \end{pmatrix}\begin{pmatrix} U1 \\ U2 \end{pmatrix}; \\[2mm] V(\zeta) = \begin{pmatrix} N_{1V} & N_{2V} \end{pmatrix}\begin{pmatrix} V1 \\ V2 \end{pmatrix}; \\[2mm] \theta(\zeta) = \begin{pmatrix} N_{1\theta} & N_{2\theta} \end{pmatrix}\begin{pmatrix} \theta1 \\ \theta2 \end{pmatrix} \end{cases} \tag{17}$$

In order to have more accurate results, shape functions are supposed to be harmonic:

$$\begin{cases} N_{1U} = \dfrac{\sin(\sigma(1-\zeta))}{\sin\sigma}; \\[2mm] N_{2U} = \dfrac{\sin(\sigma\zeta)}{\sin\sigma}; \\[2mm] N_{1V} = \dfrac{\sin(\eta(1-\zeta))}{\sin\eta}; \\[2mm] N_{2V} = \dfrac{\sin(\eta\zeta)}{\sin\eta}; \\[2mm] N_{1\theta} = \dfrac{\sin(\mu(1-\zeta))}{\sin\mu}; \\[2mm] N_{2\theta} = \dfrac{\sin(\mu\zeta)}{\sin\mu} \end{cases} \tag{18}$$

Substituting the above shape functions in the virtual work formulations results in:

$$W_U^e = \begin{pmatrix} \delta U_1 & \delta U_2 \end{pmatrix}\left(\dfrac{k_{11}}{l}\begin{bmatrix} -N_{1U,\zeta=0}' & N_{1U,\zeta=1}' \\ -N_{2U,\zeta=0}' & N_{2U,\zeta=1}' \end{bmatrix}\begin{pmatrix} U_1 \\ U_2 \end{pmatrix}\right.$$
$$+\dfrac{k_{12}}{l}\int\limits_0^1\begin{bmatrix} N_{1U}'N_{1V}' & N_{1U}'N_{2V}' \\ N_{2U}'N_{1V}' & N_{2U}'N_{2V}' \end{bmatrix}d\zeta\begin{pmatrix} V_1 \\ V_2 \end{pmatrix}+$$
$$\dfrac{k_{13}}{l}\int\limits_0^1\begin{bmatrix} N_{1U}'N_{1\theta}' & N_{1U}'N_{2\theta}' \\ N_{2U}'N_{1\theta}' & N_{2U}'N_{2\theta}' \end{bmatrix}d\zeta\begin{pmatrix} \theta_1 \\ \theta_2 \end{pmatrix};$$
$$W_V^e = \begin{pmatrix} \delta V_1 & \delta V_2 \end{pmatrix}\left(\dfrac{k_{22}}{l}\begin{bmatrix} -N_{1V,\zeta=0}' & N_{1V,\zeta=1}' \\ -N_{2V,\zeta=0}' & N_{2V,\zeta=1}' \end{bmatrix}\begin{pmatrix} V_1 \\ V_2 \end{pmatrix}\right.+$$
$$\dfrac{k_{21}}{l}\int\limits_0^1\begin{bmatrix} N_{1V}'N_{1U}' & N_{1V}'N_{2U}' \\ N_{2V}'N_{1U}' & N_{2V}'N_{2U}' \end{bmatrix}d\zeta\begin{pmatrix} U_1 \\ U_2 \end{pmatrix}+$$
$$\dfrac{k_{23}}{l}\int\limits_0^1\begin{bmatrix} N_{1V}'N_{1\theta}' & N_{1V}'N_{2\theta}' \\ N_{2V}'N_{1\theta}' & N_{2V}'N_{2\theta}' \end{bmatrix}d\zeta\begin{pmatrix} \theta_1 \\ \theta_2 \end{pmatrix};$$
$$W_\theta^e = \begin{pmatrix} \delta\theta_1 & \delta\theta_2 \end{pmatrix}\left(\dfrac{k_{33}}{l}\begin{bmatrix} -N_{1\theta,\zeta=0}' & N_{1\theta,\zeta=1}' \\ -N_{2\theta,\zeta=0}' & N_{2\theta,\zeta=1}' \end{bmatrix}\begin{pmatrix} \theta_1 \\ \theta_2 \end{pmatrix}\right.+$$
$$\dfrac{k_{31}}{l}\int\limits_0^1\begin{bmatrix} N_{1\theta}'N_{1U}' & N_{1\theta}'N_{2U}' \\ N_{2\theta}'N_{1U}' & N_{2\theta}'N_{2U}' \end{bmatrix}d\zeta\begin{pmatrix} U_1 \\ U_2 \end{pmatrix}+$$
$$\dfrac{k_{32}}{l}\int\limits_0^1\begin{bmatrix} N_{1\theta}'N_{1V}' & N_{1\theta}'N_{2V}' \\ N_{2\theta}'N_{1V}' & N_{2\theta}'N_{2V}' \end{bmatrix}d\zeta\begin{pmatrix} V_1 \\ V_2 \end{pmatrix} \tag{19}$$

And so by defining the movement vector of the elements as:

$$a = \{U_1; U_2; V_1; V_2; \theta_1; \theta_2\}^T \tag{20}$$

Stiffness matrix of the whole system can be calculated as:

$$K_T = \begin{bmatrix} K_{11} & K_{12} & K_{13} \\ K_{21} & K_{22} & K_{23} \\ K_{31} & K_{32} & K_{33} \end{bmatrix} =$$

$$K_{11} = \frac{k_{11}}{l}\begin{bmatrix} -N'_{1U,\zeta=0} & N'_{1U,\zeta=1} \\ -N'_{2U,\zeta=0} & N'_{2U,\zeta=1} \end{bmatrix}d\zeta \quad K_{12} = \frac{k_{12}}{l}\int_0^1 \begin{bmatrix} N'_{1U}N'_{1V} & N'_{1U}N'_{2V} \\ N'_{2U}N'_{1V} & N'_{2U}N'_{2V} \end{bmatrix}d\zeta \ (21)$$

$$K_{13} = \frac{k_{13}}{l}\int_0^1 \begin{bmatrix} N'_{1U}N'_{1\theta} & N'_{1U}N'_{2\theta} \\ N'_{2U}N'_{1\theta} & N'_{2U}N'_{2\theta} \end{bmatrix}d\zeta \quad K_{21} = \frac{k_{21}}{l}\int_0^1 \begin{bmatrix} N'_{1V}N'_{1U} & N'_{1V}N'_{2U} \\ N'_{2V}N'_{1U} & N'_{2V}N'_{2U} \end{bmatrix}d\zeta$$

$$K_{22} = \frac{k_{22}}{l}\begin{bmatrix} -N'_{1V,\zeta=0} & N'_{1V,\zeta=1} \\ -N'_{2V,\zeta=0} & N'_{2V,\zeta=1} \end{bmatrix}d\zeta \quad K_{23} = \frac{k_{23}}{l}\int_0^1 \begin{bmatrix} N'_{1V}N'_{1\theta} & N'_{1V}N'_{2\theta} \\ N'_{2V}N'_{1\theta} & N'_{2V}N'_{2\theta} \end{bmatrix}d\zeta$$

$$K_{31} = \frac{k_{31}}{l}\int_0^1 \begin{bmatrix} N'_{1\theta}N'_{1U} & N'_{1\theta}N'_{2U} \\ N'_{2\theta}N'_{1U} & N'_{2\theta}N'_{2U} \end{bmatrix}d\zeta \quad K_{32} = \frac{k_{32}}{l}\int_0^1 \begin{bmatrix} N'_{1\theta}N'_{1V} & N'_{1\theta}N'_{2V} \\ N'_{2\theta}N'_{1V} & N'_{2\theta}N'_{2V} \end{bmatrix}d\zeta$$

$$K_{33} = \frac{k_{33}}{l}\begin{bmatrix} -N'_{1\theta,\zeta=0} & N'_{1\theta,\zeta=1} \\ -N'_{2\theta,\zeta=0} & N'_{2\theta,\zeta=1} \end{bmatrix}d\zeta$$

4   ANSYS MODELING

A. MODELING OF PLANAR ROBOT

Based on the mentioned formulations, two cases of the cable robots are simulated in ANSYS software and their natural frequencies and mode shapes are gained. The first structure is a planar cable robot with three cables and two degrees of freedom like Fig. 3. Here two DOFs of the lumped mass of m (X, Y) are controlled using three flexible cables with time dependent length of L_i which are connected to three fixed drums of inertia J_i and rotational damping coefficient of c_i at the position of A_i with the angle of θ_i. The distance of the drums is L_B.
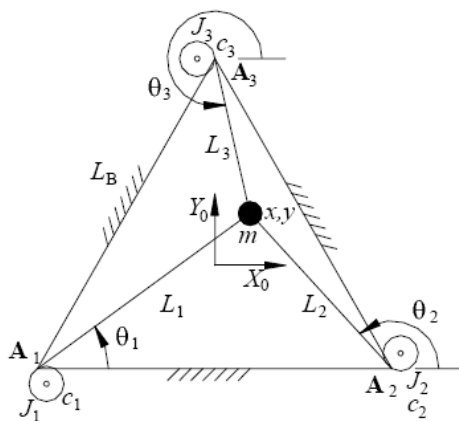
Fig. 3   Schematic of a planar cable robot [16]

This structure is modelled in ANSYS by making full constraint in the triangular shaped frame and also making z direction constraint for the cables movement in order to study their planar vibration (Fig. 4), where the related parameters are presented in Table 1.

TABLE 1 PARAMETERS OF PLANAR MODELING

Analysis Type	Structural Modal Sub-space
Element type	PIPE16
Outside diameter	0.04 unit
Wall thickness	0.02 unit
Pipe wall mass	0.03 unit
Pipe axial stiffness	4.5×10^6 unit
Material properties	Linear Elastic Isotrop $E=4.5\times10^6$ unit, $\upsilon=0.3$
Mesh type	Line Mesh
Key Point1	(1,0,0)
Key Point2	(-1,0,0)
Key Point3	(0,2,0)
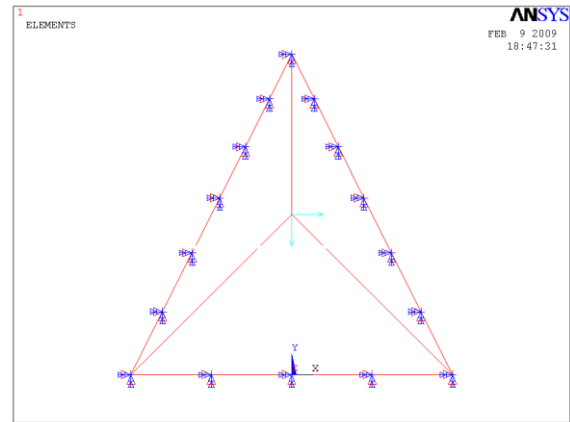
Fig. 4   ANSYS model of the planar cable robot
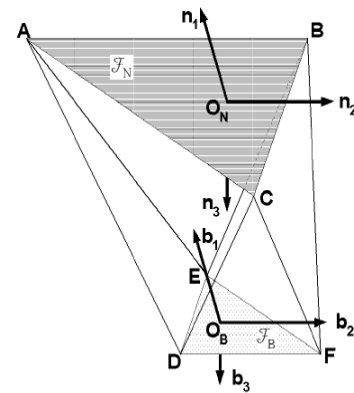
Fig. 5   Schematic of a spatial cable robot [19]

B. MODELING OF SPATIAL ROBOT

In the second case there is a spatial cable robot with six cables and six degrees of freedom for the triangular shaped end-effector as illustrated in Fig. (5). Here F_n is

the fixed global coordinate attached to the fixed upper plate of the robocrane, F_b is local coordinate of the moving end-effector, A,B,C are the corners of the fixed plate and E,D,F are the corners of the moving end-effector and these points are connected using six flexible cables of time dependent length. The base triangle is constrained in all of its degrees of freedom and the end effector is free to vibrate through the cables (Fig. 6):
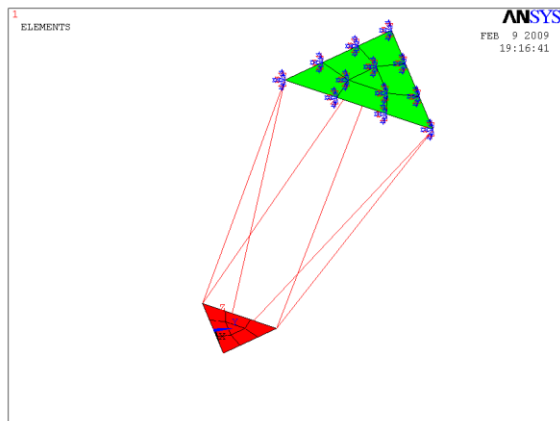
Fig. 6　　ANSYS model of a spatial cable robot

Related parameters can be found in Table 2:

TABLE 2: PARAMETERS OF SPATIAL MODELING

Analysis Type	Structural Modal Sub-space
Element type	PIPE16
Outside diameter	0.04 unit
Wall thickness	0.02 unit
Pipe wall mass	0.03 unit
Pipe axial stiffness	4.5×10^6 unit
Material properties	Linear Elastic Isotrop $E=4.5 \times 10^6$ unit, $\upsilon=0.3$
Mesh type	$\begin{cases} \text{cables:Line mesh} \\ \text{plates:Triangular} \end{cases}$
Distance between base and end-effector	10 units
End-effector	$\begin{cases} \text{Key-point1:}(1,0,0) \\ \text{Key-point2:}(-1,0,0) \\ \text{Key-point3:}(0,2,0) \end{cases}$
Base	$\begin{cases} \text{Key-point1:}(2,3,10) \\ \text{Key-point2:}(-2,3,10) \\ \text{Key-point3:}(0,-1,10) \end{cases}$

5　SIMULATION STUDY

A. SIMULATION OF PLANAR ROBOT

Using the mentioned parameters results in the following nodal mode shape functions of Fig. 7 and frequencies of Table 3:
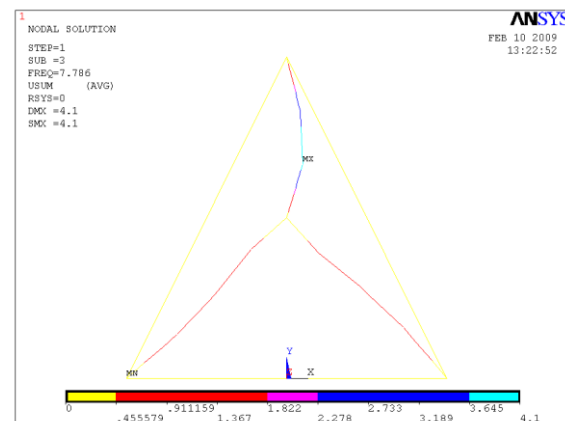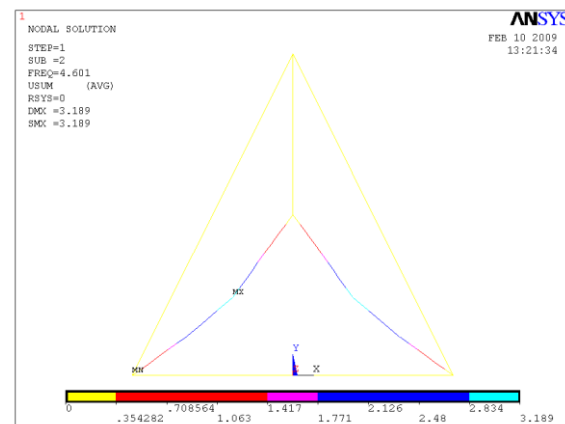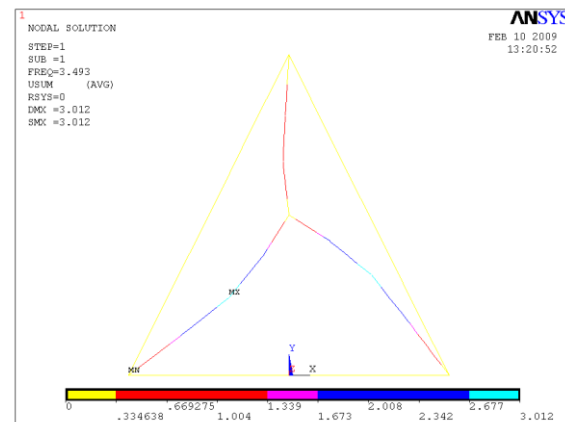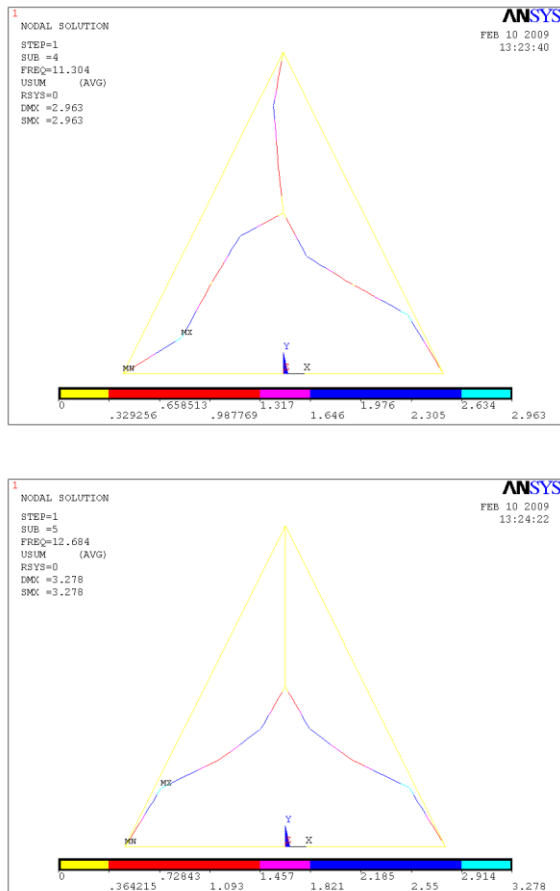
Fig. 7   First five mode shapes of the planar system

TABLE 3: FIRST TEN NATURAL FREQUENCIES OF THE PLANAR ROBOT

Step	Time (sec)/Frequency(Hz)
1	3.4929
2	4.6014
3	7.7857
4	11.304
5	12.684
6	21.047
7	24.809
8	25.284
9	40.357
10	40.773

It can be seen that the critical vibrations are occurred at the middle of the cables and as a result, it does not critically affect the position of the end-effector. The critical vibration causes significant displacement at the cables with low frequency and can be occurred easily

for a lot of boundary conditions in the case of planar robot.

Table 4: First ten natural frequencies of the flexible end-effector spatial system

Step	Time (sec)/Frequency(Hz)
1	1.1729
2	1.3359
3	1.8198
4	3.5414
5	4.2455
6	4.5021
7	11.217
8	11.807
9	15.924
10	19.306

B. SIMULATION OF SPATIAL ROBOT

Spatial simulation is done using two different conditions. First the end-effector is supposed to be elastic that its vibration is not ignorable compared to the cables' vibrations. In this condition the stress of the cables is:

```
MINIMUM VALUES
NODE      1        65        65        1         1
VALUE   0.0000   -6489.3   -24698   0.0000    0.0000


MAXIMUM VALUES
NODE     67        63        1         67        33
VALUE  25718    8198.9    0.0000   25718    23133
```

The same node numbers are related to different cables. Also the natural frequency of the whole system is presented in Table 4. First five modes of the system in nodal displacement contour are shown in Fig. 8.

In this case two categories of flexibility are observable in the mode shapes. First two modes are mostly affected by longitudinal flexibilities of the cables while the last three modes are mostly affected by lateral vibrations. It can be seen that for the cases in which the longitudinal flexibilities of the cables are ignorable compared to their lateral vibrations, the position of the end-effector is not considerably deviated while the error is not ignorable for the cases in which the longitudinal vibrations are dominant.
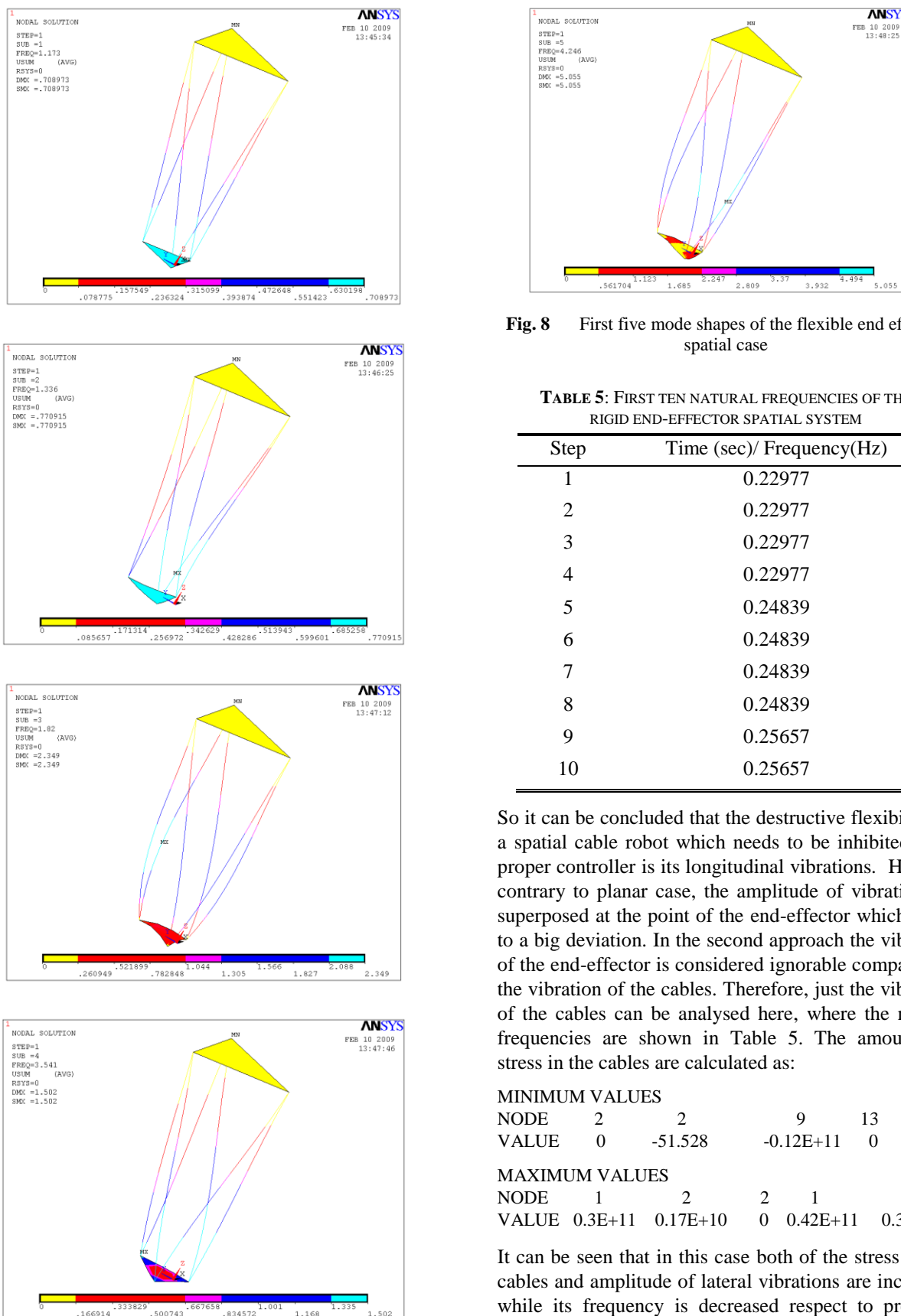
Fig. 8 First five mode shapes of the flexible end effector spatial case

TABLE 5: FIRST TEN NATURAL FREQUENCIES OF THE RIGID END-EFFECTOR SPATIAL SYSTEM

Step	Time (sec)/ Frequency(Hz)
1	0.22977
2	0.22977
3	0.22977
4	0.22977
5	0.24839
6	0.24839
7	0.24839
8	0.24839
9	0.25657
10	0.25657

So it can be concluded that the destructive flexibility of a spatial cable robot which needs to be inhibited by a proper controller is its longitudinal vibrations. Here, in contrary to planar case, the amplitude of vibrations is superposed at the point of the end-effector which leads to a big deviation. In the second approach the vibration of the end-effector is considered ignorable compared to the vibration of the cables. Therefore, just the vibration of the cables can be analysed here, where the natural frequencies are shown in Table 5. The amounts of stress in the cables are calculated as:

MINIMUM VALUES

NODE	2	2	9	13	13
VALUE	0	-51.528	-0.12E+11	0	0

MAXIMUM VALUES

NODE	1	2	2	1	1
VALUE	0.3E+11	0.17E+10	0	0.42E+11	0.39E+11

It can be seen that in this case both of the stress of the cables and amplitude of lateral vibrations are increased while its frequency is decreased respect to previous

© 2017 IAU, Majlesi Branch

study which shows that most of the vibrating energy here is consumed to vibrate the cables while for the former case, flexibility of the end-effector dissipates a section of the energy which leads to lower vibrating response of the cables. The first five modes of this system in the nodal displacement contour are shown in Fig. 9. As it was expected the end-effector is remained solid here. It can be observed that here, in contrary to flexible end-effector case most vibration of the cables are lateral which do not extremely affect the position of the end-effector.
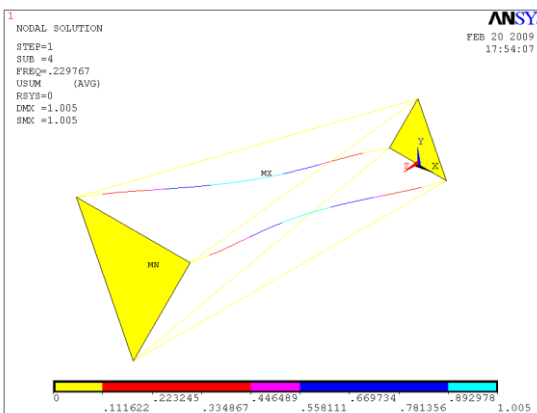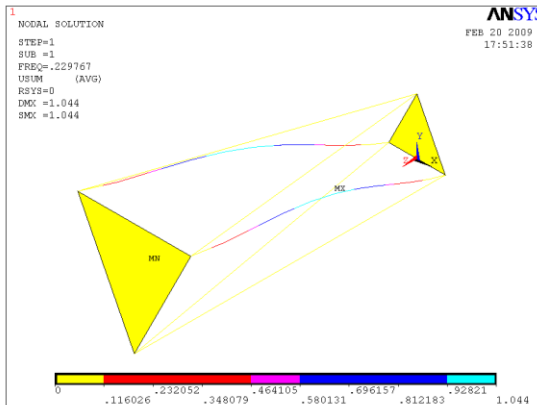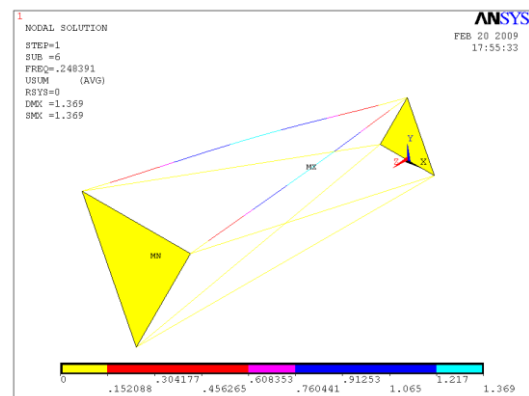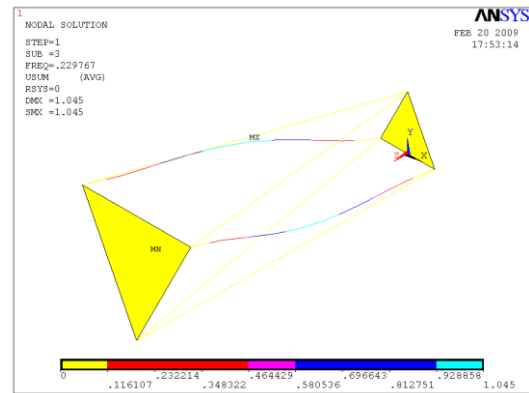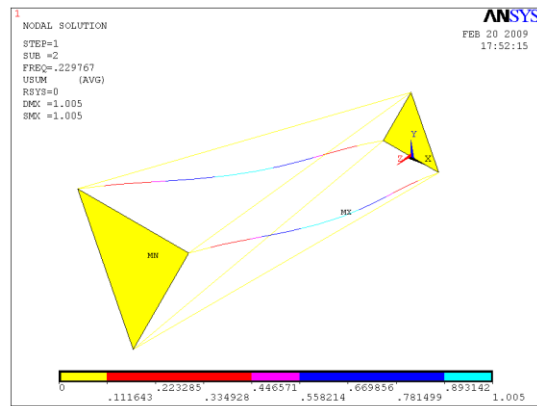
Fig. 9   First five mode shapes of the rigid end-effector spatial case

Although the amplitude of these vibrations is higher than previous case, they do not disturb the accuracy since no longitudinal flexibility is produced. So it can be concluded that providing a solid end-effector for the spatial cable robot helps its accuracy while the remained longitudinal vibrations can also be damped using a controller.

7   CONCLUSION

In this paper vibrating formulation of the cables in longitudinal, lateral and torsional directions was represented for a variable-length cable using FEM. A simulation study was done for two samples of cable structures like robocrane in which the length of the cables is time-variable. FEM was performed as a strong vibrating analyser tool for whole of the cable robot structure instead of separation analysis of each cable. Not only the 3-D vibrations of the cables were studied but also the lengths of the cables were considered variable. Results are presented for a case of planar robot with three cables and a spatial robot with six cables.

It was seen that the critical vibration by which the maximum displacement and minimum frequency is produced and can be occurred easily for a lot of boundary conditions in the case of planar robot are occurred at the middle of the cables and as a result, it does not critically effect the position of the end-effector. But the result is opposite in the case of spatial robot. In this case because of spatial structure of the robot in which the amplitude of vibrations is superposed at the point of the end-effector, an important error at the position can be observed which shows the necessity of designing a proper vibration controller. On the other hand comparing the results of solid and flexible end-effector for spatial case showed that in the case of the solid end-effector most vibrations are lateral vibration which does not cause a major displacement error in the end-effector but the amplitude and stress of the vibrations is higher and frequency of the vibrations is lower.

This is contributed to the fact that in this case all of the vibrating energy is exerted on the cables. However the vibrations in the flexible end-effector system can be dissipated by transmitting a section of vibrating energy to the end-effector and thus produces a lower amplitude and stress with bigger frequencies but because of its longitudinal nature it has more destructive effect on the position and accuracy of the system. This phenomenon shows that a solid end-effector can lead to a more accurate motion of the robot.

ACKNOWLEDGMENTS

REFERENCES

[1] Zhang, X., Mills, J. K., and Cleghorn, W. L., "Coupling Characteristics of Rigid Body Motion and Elastic Deformation of a 3-PRR Parallel Manipulator with Flexible Links", Multibody System Dynamics, Vol. 21, No. 2, 2009, pp. 167-192.

[2] Caracciolo, R., Richiedei, D. and Trevisani, A., "Experimental Validation of a Model-Based Robust Controller for Multi-Body Mechanisms with Flexible Links", Multibody System Dynamics, Vol. 20, 2008, pp. 129–145.

[3] Diao, X. and Ma, O., "Vibration Analysis of Cable-Driven Parallel Manipulators", Multibody System Dynamics, Vol. 21, No. 4, 2009, pp. 347-360.

[4] Oh, S.R., Mankala, K.K., Agrawal, S.K. and Albus, J.S., "Dynamic Modeling and Robust Controller Design of a Two-Stage Parallel Cable Robot", Multibody System Dynamics, Vol. 13, No. 4, 2005, pp. 385–399.

[5] Heyden, T. and Woernle, Ch., "Dynamics and Flatness-Based Control of a Kinematically Undetermined Cable Suspension Manipulator", Multibody System Dynamics, Vol. 16, No. 2, 2006, pp. 155-177.

[6] Kamman, J. W. and Huston, R. L., "Multibody Dynamics Modeling of Variable Length Cable Systems", Multibody System Dynamics, Vol. 5, No. 3, 2001, pp. 211-21.

[7] Yanai, N., Yamamoto, M. and Mohri, A., "Feedback Control for Wire-Suspended Mechanism with Exact Linearization", Intelligent Robots and System, IEEE/RSJ International Conference, 3, 2002, pp. 2213-2218.

[8] Fang, Sh., Franitza, D., Torlo, M., Bekes, F., and Hiller, M., "Motion Control of a Tendon-Based Parallel Manipulator Using Optimal Tension Distribution", IEEE/ASME, Transaction on Mechatronics, Vol. 9, No. 3, 2004, pp. 561 – 568.

[9] Pappas, G. J., Lygeros, J. and Godbole, D. N., "Stabilization and Tracking of Feedback Linearization Systems under Input Constarints", Intelligent Machines and Robotic Laboratory Department of Electrical Engineering and Computer Science, University of California at Berkeley, Berkeley CA-94720.

[10] Oh, S. R. and Agrawal, S. K., "Cable-Suspended Planar Parallel Robots with Redundant Cables, Controllers with Positive Cable Tensions", Mechanical Systems Laboratory, Department of Mechanical Engineering, University of Delaware, Newark, DE-19716, U.S.A, 2005.

[11] Hashemi, S. M. and Roach, A., "A Dynamic Finite Element for Vibration Analysis of a Cable and Wire Rope", Asian Journal of Civil Engineering, Vol. 7, No. 5, 2006, pp. 487-500.

[12] Wang, P. H., Fung, R. F. and Lee, M. J., "Finite Element Analysis of a Three Dimensional Underwater Cable with Time Dependent Length", Journal of Sound and Vibration, Vol. 209, No. 2, pp. 223-249, 1998.

[13] Georgakis, C. T. and Taylor, C.A., "Nonlinear Dynamics of Cable Stays", Department of Civil Engineering, Earthquake Engineering Research Center, University of Bristol, UK, Journal of Sound and Vibration, No. 281, 2005, pp. 537–564.

[14] Fung, R. F., Lul, Y. and Huang, S. C., "Dynamic Modeling and Vibration Analysis of a Flexible Cable-Stayed Beam Structure", Journal of Sound and Vibration,Vol. 254, No. 4, 2002, pp. 717–726.

[15] Williams, R. L. and Gallina, P., Rossi A., "Planar Cable Direct Driven Robots; Part 1, Kinematics and Statics", ASME Design Technical Conferences, 2001.

[16] Williams, R. L., Gallina, P. and Rossi A., "Planar Cable Direct Driven Robots; Part 2, Dynamics and control", ASME Design Technical Conferences, 2001.

[17] Alp, A. B. and Agrawal, S. K., "Cable Suspended Robots, Design, Planning and Control", Department of Mechanical Engineering, University of Delaware, Newark, DE- 19716,USA, 2001.

[18] Samaras, R.K., Skop, R.A. and Milburn, D.A., "An Analysis of Coupled Extensional-Torsional Oscillations in Wire-Rope", Transaction of the ASME, Journal of Engineering for Industry; Vol. 96, No. 4, 1974, pp. 1130-1135.

[19] Zhang Y., Agrawal S.K. and Piovoso M.J., "Coupled Dynamics of Flexible Cables and Rigid End-effector for a Cable Suspended Robot", American Control Conference, Vol. 14, No. 16, 2006.